VIP Surface Reactivity

DOI: 10.1002/anie.201106348

Ruthenium Nanoparticles Stabilized by N-Heterocyclic Carbenes: Ligand Location and Influence on Reactivity**

*Patricia Lara, Orestes Rivada-Wheelaghan, Salvador Conejero, Romuald Poteau, Karine Philippot, and Bruno Chaudret**

Despite the huge number of reports dealing with the preparation and use of metal nanoparticles (NPs), in particular for catalysis, very few are dedicated to the understanding of the surface chemistry and the influence of organic ligands, both on the chemistry and on the physics of the nanoparticles.[1] The most successful recent class of ligands in organometallic chemistry is no doubt N-heterocyclic carbenes (NHCs).[2] There are however to the best of our knowledge only three reports on the use of NHC ligands for stabilizing or modifying nanoparticles.[3–5] Among them, only that of Tilley and Vignolle reports the use of NHCs to synthesize gold NPs.[3] The others describe the addition of a chiral NHC modifier to Pd nanoparticles supported on iron oxide,[4] and the substitution of ligands by NHCs but leading to unstable particles.[5] Furthermore, two reports propose the intermediacy of NHCs in the stabilization of nanoparticles in ionic liquids.[6] None of these reports deals with the characterization of the coordination mode of the NHC ligands onto the nanoparticle surface.

Classical carbenes have been used successfully for the stabilization of ruthenium nanoparticles.[7] The NHC ligands have however many advantages, such as their strong electron-donating properties, strong binding to transition metals, absence of oxidation in contrast to for example phosphines, and the fact that they contain only C, H, and N and no other heteroatom, which makes them ideal candidates for stabilizing catalysts.[8] It is therefore astonishing not to find more examples on the use of these ligands for the stabilization of nanoparticles and is thus important to determine whether these ligands are suitable or not in this field.

We have recently developed the use of various NMR spectroscopy methods to understand the mode of coordination and the dynamics of ligands and adsorbates on the surface of nanoparticles.[9] This is in our opinion the key to control the growth and the surface state of nanoparticles, and further to obtain new selective catalysts. Thus, many in situ and operando techniques have been recently developed,[10] but alternative simple methods, similar to the molecular methods, such as NMR spectroscopy in particular, could bring additional information on the reaction sites and possibly on reaction intermediates.[9,11] For example, for ruthenium nanoparticles sterically stabilized by poly(vinylpyrrolidone) (PVP), we have determined the location and dynamics of hydrides as well as their reactivity towards olefins leading to a facile splitting of a carbon–carbon bond.[9b]

Herein we present the use of NHC ligands, namely *N*,*N*-di(*tert*-butyl)imidazol-2-ylidene (I*t*Bu; $\mathbf{L^1}$)[12] and 1,3-bis(2,6-diisopropylphenyl)imidazol-2-ylidene (IPr; $\mathbf{L^2}$)[13] to stabilize ruthenium nanoparticles (RuNPs) and the control of NHC binding by the control of the substituents on nitrogen. Furthermore, thanks to the synthesis of the analogous ligands ^{13}C-labeled on the carbene carbon, we present NMR spectroscopic evidence for NHC binding to nanoparticles, and the use of chemical reactivity (ligand exchange, CO binding, CO oxidation, styrene hydrogenation) to characterize the surface and also the location of the ligands.

Ruthenium nanoparticles were synthesized by decomposition of (1,5-cyclooctadiene)(1,3,5-cyclooctatriene)ruthenium(0) [(Ru(cod)(cot)] in pentane at room temperature under 3 bar H_2 and in the presence of variable amounts of the carbene ligands $\mathbf{L^1}$ or $\mathbf{L^2}$ (Scheme 1). The carbenes and not the imidazolium precursors are used to avoid any pollution of the nanoparticle surface. Different [ligand]/[Ru] molar ratios were tested to find the best reaction conditions to obtain well-controlled RuNPs.

Reaction of [Ru(cod)(cot)] with 0.2 equiv $\mathbf{L^1}$ leads to a black precipitate and an absence of stabilization of the nanoparticles. However, using 0.5 equiv $\mathbf{L^1}$, a brown stable colloidal solution is formed. Transmission electron microscopy (TEM) analysis revealed the presence of non-agglomerated nanoparticles of (1.7 ± 0.2) nm mean size, displaying a narrow size distribution and adopting the hcp structure of bulk ruthenium as revealed by fast Fourier transform analysis (colloid **1**, Figure 1).

[*] Dr. P. Lara, Dr. K. Philippot
CNRS; LCC (Laboratoire de Chimie de Coordination)
205 , Route de Narbonne, 31077 Toulouse (France)
and
Université de Toulouse; UPS, INPT, LCC
31077 Toulouse (France)
O. Rivada-Wheelaghan, Dr. S. Conejero
Instituto de Investigaciones Químicas-Departamento de Química Inorgánica, CSIC, Universidad de Sevilla
Avda. Américo Vespucio, 49, 41092 Sevilla (Spain)
Dr. R. Poteau, Dr. B. Chaudret
LPCNO; Laboratoire de Physique et Chimie de Nano-Objets
135, Avenue de Rangueil, 31077 Toulouse (France)
E-mail: chaudret@insa-toulouse.fr

[**] We thank V. Collière and L. Datas (UPS-TEMSCAN) and P. Lecante (CNRS-CEMES) for TEM/HR-TEM and WAXS facilities, respectively. CNRS and ANR (Siderus project ANR-08-BLAN-0010-03) are also thanked for financial support. P.L. is grateful to the Spanish Ministerio de Educación for a research contract. Financial support from the Junta de Andalucía (project no. FQM-3151) and the Spanish Ministerio de Ciencia e Innovación (projects CTQ2010-17476 and CONSOLIDER-INGENIO 2010 CSD2007-00006, FEDER support) is acknowledged. O.R.-W. thanks the Spanish Ministerio de Ciencia e Innovación for a research grant.

Supporting information for this article is available on the WWW under http://dx.doi.org/10.1002/anie.201106348.

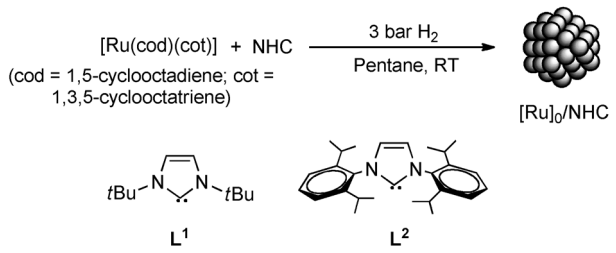

Scheme 1. The N-heterocyclic carbenes and reaction conditions used for the synthesis of ruthenium nanoparticles.

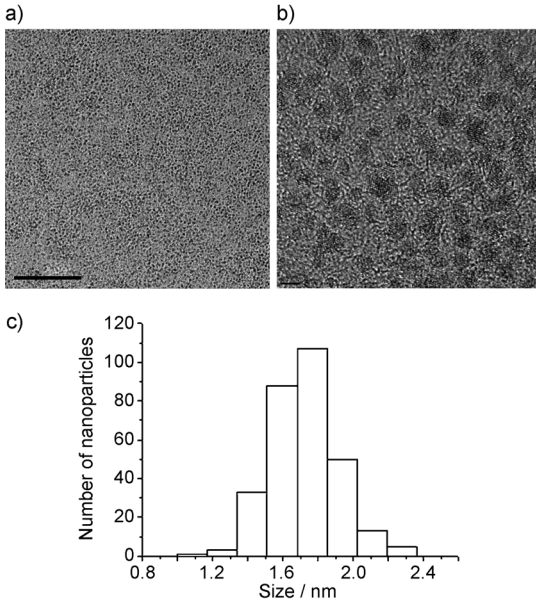

Figure 1. a) TEM image (scale bar: 50 nm) and b) HREM image (scale bar: 2 nm) with corresponding size histogram (c) of colloid **1** ([I*t*Bu]/[Ru] = 0.5).

The analogous reaction carried out in the presence of 0.2 or 0.5 equiv $\mathbf{L^2}$ leads to stable colloidal solutions in both cases (colloids **2** and **3**, respectively). TEM and HRTEM analyses revealed the presence of non-agglomerated, spherical, monodisperse, and highly crystalline nanoparticles (Supporting Information, Figures S2 and S3) with mean sizes slightly decreasing from 1.7(0.2) nm in the case of the $[\mathbf{L^2}]/[Ru] = 0.2$ system, to 1.5(0.2) for $[\mathbf{L^2}]/[Ru] = 0.5$. Higher ligand concentrations thus lead to smaller particles, as previously observed in other systems.[11b] Upon further addition of ligands (1 equiv), even smaller particles were observed (1.2 nm), but these were associated with molecular species as revealed by ^{1}H NMR spectroscopy.

An HRTEM study of colloid **3** ($[\mathbf{L^2}]/[Ru] = 0.5$) (Supporting Information, Figure S4) shows unambiguously the highly crystalline character of the particles and their hexagonal close packed structure for which fast Fourier transformation (FFT) shows reflections corresponding to the $(0\bar{1}11)$, $(1\bar{1}01)$, and $(10\bar{1}0)$ atomic planes. The hcp structure of the different colloids is also shown by wide-angle X-ray scattering (WAXS) measurements performed on powder samples after evaporation of the solvent. Moreover, the coherence lengths of the different samples are found to be 2.0, 1.7, and 1.7 for colloids **1**, **2**, and **3** respectively, in good agreement with the mean sizes of the particles determined by HRTEM and hence with the crystalline nature of the particles.

The nanoparticles in colloids **1**–**3** are stable in solution and in the solid state in anaerobic conditions and can be handled like molecular complexes. However, colloid **1** starts precipitating after one day in solution. The surface species were studied by spectroscopic techniques as well as by titration for the surface hydrides. The latter method is based on the hydrogenation of olefins in the absence of added dihydrogen, which can thus be only induced by the existing surface hydrides (see the Supporting Information).[14] The resulting values are 1.1, 1.3, and 2.5 H/Ru$_s$ for colloids **1**, **2**, and **3**, respectively (Supporting Information, Table S2). They are in agreement with those previously found for PVP- and dppb-stabilized RuNPs.[9b,11d] The result for colloid **3** is however quite high and may result from transfer dehydrogenation of the alkyl group of $\mathbf{L^2}$ in excess, as suggested by NMR studies, in a way similar to that described originally by Crabtree to dehydrogenate alkanes.[15] This therefore leaves a surface density of hydrides and demonstrates the high reactivity of these RuNPs for hydrogen transfer.

All systems were characterized by infrared spectroscopy, for which no salient feature has been found but which confirms the presence of carbenes, as well as by solid-state and solution NMR spectroscopy (after dissolution of the particles into [D$_8$]toluene for the latter). The ^{1}H NMR spectrum of colloid **1** only shows a broad signal around 1.4 ppm attributed to the *t*Bu groups but no signals in the 6–7 ppm region where the C*H* protons of the imidazole backbone are expected. The absence of signals for groups immobilized close to nanoparticle surfaces has previously been observed by solution NMR spectroscopy.[11b,16,17] It is characteristic of the coordination of the ligands at the surface of the particles and results both from the slow tumbling of the particles in solution leading to fast T_2 relaxation and from surface heterogeneities.[18] Such a phenomenon has also been observed by Tilley and Vignolle in the characterization of NHC-stabilized gold nanoparticles.[3] In the case of colloid **2**, no signals corresponding to the aromatic protons of the phenyl rings, the C*H* imidazole protons, and the isopropyl CH proton ($CH(CH_3)_2$) groups are visible. A very broad signal is only discernable in the 1.0–1.8 ppm region for the methyl groups together with some hydrogenated carbene, as in colloid **1**. The analysis of the ^{1}H NMR spectrum of colloid **3** leads to the same conclusion. These observations demonstrate the rigidity of the coordination of both $\mathbf{L^1}$ and $\mathbf{L^2}$ carbene ligands on the ruthenium surface. Furthermore, in the case of colloid **2**, it suggests a close proximity of the phenyl rings to the surface of the particles and possibly their participation in the stabilization of the nanoparticles through a π or an agostic interaction. We previously observed a similar NMR behavior in the case of RuNPs stabilized with the 4-(3-phenylpropyl)-pyridine for which π coordination of the phenyl ring was demonstrated.[17]

To evaluate the strength of the interaction between the carbene ligands and the surface of the nanoparticles, ligand substitution was attempted by adding an excess of good σ-donor ligands, such as diphenylphosphinobutane or dodeca-

nethiol directly in a [D_8]toluene solution of colloids **1** and **2**. This reaction was followed by ^{1}H NMR. The addition of diphenylphosphinobutane to colloids **1** and **2** and of dodecanethiol to colloid **1** only showed the signals for the free added ligands (diphosphine or thiol) and no evidence either for the coordination of such ligands or for free $\mathbf{L^1}$ or $\mathbf{L^2}$ in solution. This result confirms that the carbenes are firmly coordinated to the ruthenium surface, in good agreement with the known strong bonds that NHCs form with metal complexes.[19]

The coordination of the carbene ligands $\mathbf{L^1}$ and $\mathbf{L^2}$ on the surface was studied by solid-state NMR at magic-angle spinning (MAS-NMR) with and without ^{1}H–^{13}C cross-polarization (CP) with the aim of determining their location and possible dynamics. The CP MAS spectrum of colloid **1** shows two broad signals near 120 and 55 ppm attributed to the (*C*HN) and (-*C*$(CH_3)_3$) groups of $\mathbf{L^1}$, respectively, as well as a larger signal near 30 ppm for the methyl of the *t*Bu moieties (Supporting Information, Figure S5). When using $\mathbf{L^1}$ ^{13}C labeled on the carbene carbon ($\mathbf{L^1}$*), the spectrum of the corresponding colloid, **1***, shows a broad peak centered at 190 ppm that is attributed to the coordinated carbene function. Colloids **2** and **3** only show a broad signal near 25 ppm for the *i*Pr carbon atoms and peaks near 125 ppm and 135–150 ppm for the aromatic carbon atoms. However, when using a labeled ligand ($\mathbf{L^2}$*, colloid **2***), the coordination of the carbene carbon was observed at 205 ppm (Figure 2).

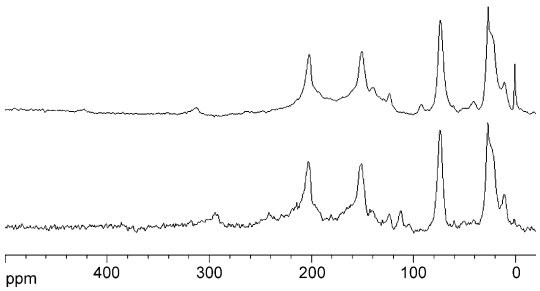

Figure 2. ^{13}C MAS (bottom) and CP-MAS (top) NMR spectra of colloid **2*** (^{13}C-labeled [IPr]/[Ru] = 0.2 NPs).

Lower chemical shifts of the carbene carbon atom in the ^{13}C NMR are consistent with ligand coordination to transition metals.[20] Interestingly, for colloid **3*** which contains excess $\mathbf{L^2}$*, besides the signal at 205 ppm, another one appears at 195 ppm which does not correspond to the free ligand (216 ppm). The presence of these two signals suggests different chemical environments for the carbene ligand $\mathbf{L^2}$*, which could result from coordination at two different ruthenium sites (Figure 3).

To probe the free sites present on the particle surfaces, ^{13}CO was added to solid samples of colloids **1**–**3** under mild conditions (room temperature, 0.5 or 0.6 atm). In the case of colloid **1**, the ^{13}C MAS NMR spectrum shows an intense and very broad signal for bridging carbonyl groups centered at 240 ppm, with no apparent spinning sideband and a weaker but sharper signal near 200 ppm with spinning sidebands corresponding to nondiffusing terminal carbonyl groups.

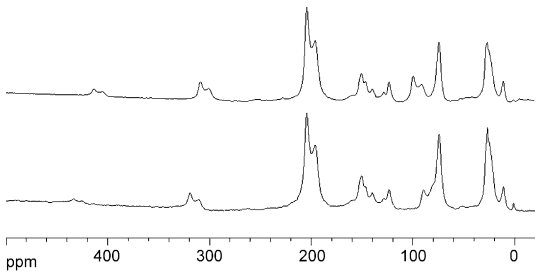

Figure 3. ^{13}C MAS (bottom) and CP-MAS (top) NMR spectra of colloid **3*** (^{13}C-labeled [IPr]/[Ru] = 0.5 NPs).

Using the CP-MAS technique, the intensity of the terminal CO signal increases (Figure 4). This indicates their location in the vicinity of hydrogen carriers, namely the $\mathbf{L^1}$ carbene

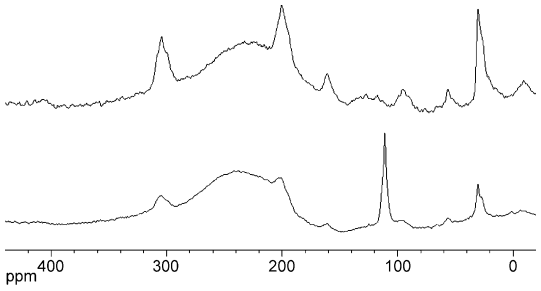

Figure 4. ^{13}C MAS (bottom) and CP-MAS (top) NMR spectra of colloid **1** after exposure to a ^{13}CO atmosphere (0.6 bar, 20 h, RT).

ligands. Addition of ^{13}CO was also performed on colloids **2** and **3** (or colloids **2*** and **3***) prepared in the presence of 0.2 or 0.5 equiv of ligand $\mathbf{L^2}$ (or labeled $\mathbf{L^2}$*), respectively. For colloid **2**, a spectrum similar to that of colloid **1** is observed, namely a broad bridging CO signal centered at 240 ppm and rigid terminal CO groups located near hydrogen carriers and overlapping with the carbene signal in the case of colloid **2*** (Supporting Information, Figure S13). However, for colloids **3** (Figure 5) or **3***, only static terminal CO signals are observed and no (or very little) bridging CO (Supporting Information, Figures S7 and S12). Furthermore, at room temperature, Colloid **1** + CO burns in air, Colloid **2** + CO is degraded in air leading to CO oxidation, and colloid **3** + CO reacts very slowly with dioxygen in air. This provides evidence for the ability of ruthenium nanoparticles to oxidize CO under mild conditions and also suggests in the case of colloid **3** the deactivation of the reactive faces after coordination of the

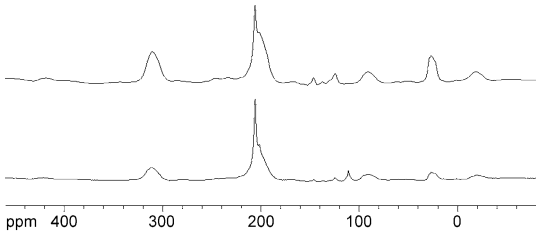

Figure 5. ^{13}C MAS (bottom) and CP-MAS (top) NMR spectra of colloid **3** after exposure to a ^{13}CO atmosphere (0.5 bar, 20 h, RT).

carbene ligand. The terminal CO groups on the edges are not oxidized.

A typical test reaction for ruthenium nanoparticles is arene hydrogenation. The reaction was carried out at room temperature in THF in the presence of 3 bar H_2 and for a [substrate]/[catalyst] molar ratio of 315 using colloid **1** or colloid **3** as catalysts. In both cases, the reaction proceeds as expected, with full hydrogenation of the vinyl bond initially, followed by hydrogenation of ethylbenzene into ethylcyclohexane. The rates are similar for both colloids but significantly slower than for a simple Ru/PVP system, thus suggesting a reactivity limitation owing to ruthenium surface covering by the carbene ligands (see the Supporting Information).

This set of reactions demonstrates the high affinity of carbene ligands for ruthenium nanoparticles. The nanoparticles are stable in solution and can be used for catalytic reactions. They do not show any sign of fluxionality or ligand dissociation in THF by ^{1}H NMR spectroscopy, and the carbene ligands are not displaced in solution by diphosphines or thiols. As expected, the carbenes first coordinate on the most exposed atoms of the particles (apexes, edges). In the case of $\mathbf{L^1}$, only the exposed ruthenium atoms can be linked to the carbene, as the bulky *t*Bu groups prevent $\mathbf{L^1}$ from coordinating to a flat surface. In contrast, it is possible to coordinate $\mathbf{L^2}$ first on the exposed atoms and on the faces. The availability of coordination sites has been tested by adding CO gas to solid samples of the different colloids. In the case of colloid **1**, the presence of almost only bridging CO reveals the absence of carbene ligand on the faces whereas the edges are encumbered by the bulky ligand. In the case of colloid **3**, in contrast, the absence of bridging CO is in agreement with the presence of carbene ligands all over the particle, although some free coordination sites for terminal CO could be found in the vicinity of the carbene ligands. Furthermore, the absence of fluxionality of the coordinated CO groups indicates that their mobility is limited by the presence of the carbene ligands. It is however possible to add sequentially the carbene ligands in the case of $\mathbf{L^2}$ leading to a selective complexation of the edges for a low $\mathbf{L^2}$ concentration and leaving the faces accessible for CO coordination. These studies therefore allow us to attain a good knowledge of the nanoparticle surface coordination chemistry. However, two facts raise questions. First, it is necessary to have an excess of ligand $\mathbf{L^1}$ to stabilize colloid **1**, which is not the case for ligand $\mathbf{L^2}$ in colloid **2**, although once coordinated, $\mathbf{L^1}$ is found only on exposed atoms and is not displaced by diphosphine or thiols. To answer this question, we have studied the hydrogenation of the carbene ligands in the presence of catalytic amount of [Ru(cod)(cot)] or of preformed colloids. We found that $\mathbf{L^1}$ is easily hydrogenated at room temperature under 3 bar H_2, first into the unsaturated substituted 1,3-diazacyclopentene and then into the corresponding 1,3-diazacyclopentane. This reaction transforming the carbene carbon into a hydrogen saturated aliphatic carbon has been observed previously during hydrogenation of a bis(carbene)palladium(0) complex, although the role of palladium black formed in this process has not been clarified.[21] In addition, this reaction could explain the necessity of excess $\mathbf{L^1}$ to obtain stable RuNPs, as we checked that the products of hydrogenation do not stabilize nanoparticles. However, no hydrogenation (or a very limited amount) is observed with $\mathbf{L^2}$. It is not clear why, but it may result either from an electronic effects (less-basic substituents on nitrogen and stabilization by conjugation in the case of $\mathbf{L^2}$) or from a stabilization of the structure by ring–metal interactions. The second point concerns styrene hydrogenation, which is achieved at comparable rates for colloids **1** and **3**. This reaction requires the π coordination of the aromatic rings on the nanoparticle faces, which, in the case of colloid **3**, are not accessible to CO in a gas–solid reaction. It is however likely that in solution styrene may displace the possible π interactions developed by the phenyl rings of $\mathbf{L^2}$.[22]

In conclusion, we have presented the synthesis of stable ruthenium nanoparticles using carbene ligands. Thanks to NMR spectroscopy studies on the ^{13}C labeling of the carbenes and to the addition of ^{13}CO, we observed the strong binding of the NHC ligands to the surface and were able to propose a location for them on the particles. Furthermore, we provide evidence for the influence of the substituents of the carbenes on the reactivity of the nanoparticles, which is mainly due to steric effects. This study therefore describes new organometallic objects covered by different species: hydrides, CO, carbenes that can be located, the dynamics of which can be studied, and which behave differently as a function of their location on the particles (Figure 6). It is therefore an attempt at the full molecular characterization of the surface of catalytically active nanoparticles.

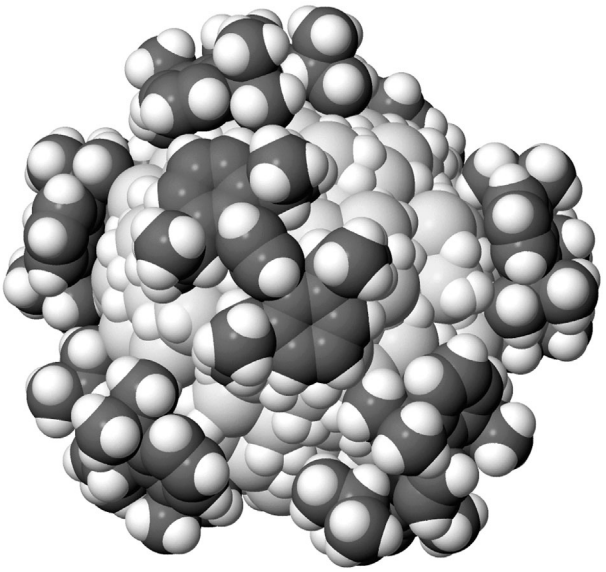

Figure 6. Space-filling model of a 1.8 nm hcp Ru nanoparticle stabilized by 8 $\mathbf{L^2}$ NHC ligands and accommodating 1.5 hydrides per surface Ru.

Received: September 7, 2011
Published online: October 28, 2011

Keywords: nanoparticles · N-heterocyclic carbenes · ruthenium · solid-state NMR spectroscopy · surface reactivity

[1] a) *Clusters and Colloids. From Theory to Applications* (Ed.: G. Schmid), Wiley-VCH, Weinheim, **1994**; *Nanoparticles. From Theory to Application* (Ed: G. Schmid), Wiley-VCH, Weinheim, **2004**; b) A. Roucoux, K. Philippot in *Handbook of Homogeneous Hydrogenations*, *Vol. 9* (Eds: J. G. de Vries, C. J. Elsevier), Wiley-VCH, Weinheim, **2007**, pp. 217 – 255; c) *Nanoparticles and Catalysis* (Ed.: D. Astruc), WILEY-INTERSCIENCE, New York, **2008**.

[2] a) F. E. Hahn, M. C. Jahnke, *Angew. Chem.* **2008**, *120*, 3166 – 3216; *Angew. Chem. Int. Ed.* **2008**, *47*, 3122 – 3172; b) N. M. Scott, S. P. Nolan, *Eur. J. Inorg. Chem.* **2005**, 1815 – 1828; c) O. Schuster, L. Yang, H. G. Raubenheimer, M. Albrecht, *Chem. Rev.* **2009**, *109*, 3445 – 3478; d) P. L. Arnold, I. J. Casely, *Chem. Rev.* **2009**, *109*, 3599 – 3611; e) M. Poyatos, J. A. Mata, E. Peris, *Chem. Rev.* **2009**, *109*, 3677 – 3707.

[3] J. Vignolle, T. D. Tilley, *Chem. Commun.* **2009**, 7230 – 7232.

[4] K. V. S. Ranganath, J. Kloesges, A. S. Schäfer, F. Glorius, *Angew. Chem.* **2010**, *122*, 7952 – 7956; *Angew. Chem. Int. Ed.* **2010**, *49*, 7786 – 7789.

[5] E. C. Hurst, K. Wilson, I. J. S. Fairlamb, V. Chechik, *New J. Chem.* **2009**, *33*, 1837 – 1840.

[6] a) L. S. Ott, M. L. Cline, M. Deetlefs, K. R. Seddon, R. G. Finke, *J. Am. Chem. Soc.* **2005**, *127*, 5758 – 5759; b) J. D. Scholten, G. Ebeling, J. Dupont, *Dalton Trans.* **2007**, 5554 – 5560.

[7] C. Wei, J. R. Davies, D. Gosh, M. C. Tog, J. P. Konopelski, S. Wie, *Chem. Mater.* **2006**, *18*, 5253 – 5259.

[8] a) S. Díez-González, N. Marion, S. P. Nolan, *Chem. Rev.* **2009**, *109*, 3612 – 3676; b) R. H. Crabtree, *J. Organomet. Chem.* **2005**, *690*, 5451 – 5457; c) T. Dröge, F. Glorius, *Angew. Chem.* **2010**, *122*, 7094 – 7107; *Angew. Chem. Int. Ed.* **2010**, *49*, 6940 – 6952; d) M. Melaimi, M. Soleilhavoup, G. Bertrand, *Angew. Chem.* **2010**, *122*, 8992 – 9032; *Angew. Chem. Int. Ed.* **2010**, *49*, 8810 – 8849; e) D. G. Gusev, *Organometallics* **2009**, *28*, 6458 – 6461; f) T. Strassner, *Top. Organomet. Chem.* **2007**, *22*, 125 – 148.

[9] a) T. Pery, K. Pelzer, G. Buntkowski, K. Philippot, H. H. Limbach, B. Chaudret, *ChemPhysChem* **2005**, *6*, 605 – 607; b) J. García-Antón, M. R. Axet, S. Jansat, K. Philippot, B. Chaudret, T. Pery, G. Buntkowsky, H. H. Limbach, *Angew. Chem.* **2008**, *120*, 2104 – 2108; *Angew. Chem. Int. Ed.* **2008**, *47*, 2074 – 2078; c) L. A. Truflandier, I. Del Rosal, B. Chaudret, R. Poteau, I. C. Gerber, *ChemPhysChem* **2009**, *10*, 2939 – 2942.

[10] a) A. Zecchina, E. Groppo, S. Bordiga, *Chem. Eur. J.* **2007**, *13*, 2240 – 2460; b) G. A. Somorjai, H. Frei, J. Y. J. Park, *J. Am. Chem. Soc.* **2009**, *131*, 16589 – 16605; c) B. M. Weckhuysen, *Chem. Soc. Rev.* **2010**, *39*, 4557 – 4559; d) H. Topsøe, *J. Catal.* **2003**, *216*, 155 – 164.

[11] a) K. Philippot, B. Chaudret, *C. R. Chim.* **2003**, *6*, 1019 – 1034; b) C. Pan, K. Pelzer, K. Philippot, B. Chaudret, F. Dassenoy, P. Lecante, M.-J. Casanove, *J. Am. Chem. Soc.* **2001**, *123*, 7584 – 7593; c) M. Guerrero, J. García-Antón, M. Tristany, J. Pons, K. Philippot, P. Lecante, B. Chaudret, *Langmuir* **2010**, *26*, 15532 – 15540; d) F. Novio, K. Philippot, B. Chaudret, *Catal. Lett.* **2010**, *140*, 1 – 7.

[12] N. M. Scott, R. Dorta, E. D. Stevens, A. Correa, L. Cavallo, S. P. Nolan, *J. Am. Chem. Soc.* **2005**, *127*, 3516 – 3526.

[13] L. Jafarpour, E. D. Stevens, S. P. Nolan, *J. Organomet. Chem.* **2000**, *606*, 49 – 54.

[14] F. Humblot, D. Didillon, F. Lepeltier, J. P. Candy, J. P. Corker, O. Clause, F. Bayard, J. M. Basset, *J. Am. Chem. Soc.* **1998**, *120*, 137 – 146.

[15] R. H. Crabtree, *Chem. Rev.* **1985**, *85*, 245 – 269.

[16] a) R. H. Terrill, T. A. Postlethwaite, C.-H. Chen, C.-D. Poon, A. Terzis, A. Chen, J. E. Hutchison, M. R. Clark, G. Wignall, J. D. Londono, R. Superfine, M. Falvo, C. S. Johnson, Jr., E. T. Samulski, R. W. Murray, *J. Am. Chem. Soc.* **1995**, *117*, 12537 – 12548; b) A. Badia, W. Gao, S. Singh, L. Demers, L. Cuccia, L. Reven, *Langmuir* **1996**, *12*, 1262 – 1269.

[17] I. Favier, S. Massou, E. Teuma, K. Philippot, B. Chaudret, M. Gómez, *Chem. Commun.* **2008**, 3296 – 3298.

[18] a) E. Ramírez, L. Eradès, K. Philippot, P. Lecante, B. Chaudret, *Adv. Funct. Mater.* **2007**, *17*, 2219 – 2228; b) E. Ramírez, S. Jansat, K. Philippot, P. Lecante, M. Gómez, A. M. Masdeu-Bultó, B. Chaudret, *J. Organomet. Chem.* **2004**, *689*, 4601 – 4610.

[19] H. Jacobsen, A. Correa, A. Poater, C. Costabile, L. Cavallo, *Coord. Chem. Rev.* **2009**, *253*, 687 – 703.

[20] D. Tapu, D. A. Dixon, C. Roe, *Chem. Rev.* **2009**, *109*, 3385 – 3407.

[21] P. L. Arnold, F. G. N. Cloke, T. Geldbach, P. B. Hitchcock, *Organometallics* **1999**, *18*, 3228 – 3233.

[22] S. Würtz, F. Glorius, *Acc. Chem. Res.* **2008**, *41*, 1523 – 1533.

